Supramolecular Chemistry
Publication details, including instructions for authors and subscription information:
http://www.informaworld.com/smpp/title~content=t713649759

Intelligent compounds which read DNA base sequences

Reiko Kuroda[a]; H. Tanaka[a]; H. Satoh[a]; M. Shinomiya[a]; T. Amagai[a]; M. Furubayashi[a]
[a] Department of Chemistry, College of Arts and Sciences, The University of Tokyo, Tokyo, Japan

To cite this Article Kuroda, Reiko , Tanaka, H. , Satoh, H. , Shinomiya, M. , Amagai, T. and Furubayashi, M.(1995) 'Intelligent compounds which read DNA base sequences', Supramolecular Chemistry, 6: 1, 95 — 102
To link to this Article: DOI: 10.1080/10610279508032524
URL: http://dx.doi.org/10.1080/10610279508032524

SUPRAMOLECULAR CHEMISTRY, Vol. 6, pp. 95–102
Reprints available directly from the publisher
Photocopying permitted by license only

Intelligent compounds which read DNA base sequences

REIKO KURODA*, H. TANAKA, H. SATOH, M. SHINOMIYA, T. AMAGAI and M. FURUBAYASHI

Department of Chemistry, College of Arts and Sciences, The University of Tokyo, Komaba, Meguro, Tokyo 153, Japan

(Received August 5, 1994)

We have studied the DNA binding and DNA cleavage specificities of two novel classes of synthetic DNA breakage agents. One class comprises redox-activated metalloporphyrins, the other uses the photoactivable *p*-nitrobenzoyl group as the DNA breaking moiety linked covalently to a DNA recognizing entity such as an oligo *N*-methylpyrrolecarboxamide or oligothiazole group. Studies of DNA cleavage using end-labeled DNA restriction fragments and high resolution sequencing gel electrophoresis have allowed DNA break sites to be identified at the nucleotide level. This work in conjunction with induced CD spectroscopy has shown that these compounds, especially photoactive agents containing thiazole units, display high sequence specificity. The mechanism of sequence recognition appears to be quite different for the two series of compounds.

INTRODUCTION

DNA sequence recognition plays a key role in many biologically important processes. Gene expression, for example, is controlled by binding of repressor proteins or RNA polymerase to certain regions of DNA. The restriction enzymes display a stringent sequence preference and cleave DNA at a specific bond by recognizing a four or six base-pair (bp) sequence. To understand the interactions which underlie these biological processes, studies of small molecule–DNA interactions are particularly useful as such systems can provide information at the molecular level. We have designed and synthesized compounds of small molecular weight which recognize DNA base sequence and cleave DNA in a highly sequence specific manner.

Two types of compounds, *i.e.*, photoactive and redox-active compounds have been studied (Fig. 1). The photoactive compounds (Fig. 1a) are based on the linkage of a DNA cleaving and a DNA binding domain to a group which is expected to recognize DNA base sequence. The *p*-nitrobenzoyl group at one end of these molecules mediates DNA breakage on UV irradiation, while an intercalator or a group containing positive charges at the other end enhances the compounds's affinity toward DNA. Series 1 compounds are reference compounds, and the two functional groups are linked to a hexamethylene chain which will not recognize DNA base sequences.[1] In contrast, for compounds of series 2 and 3, a third moiety which recognizes DNA base sequences was attached. The group for series 2 is a component of the DNA-binding antibiotics netropsin/distamycin[2] which have been reported to exhibit some preference towards AT bases.[3] Compounds of series 3, on the other hand, contain thiazole groups which are a component of the bleomycin anticancer antibiotics. Compounds 3, 3L and 4, 4L contain two and three *N*-methylpyrrolecarboxamide groups, respectively. Similarly, compounds 5, 6 and 7 have two, one and three thiazole groups, respectively.[4] 3 and 4 of series 2 and 5A of series 3 contain a 9-aminoacridine intercalator in order to compare the sequence recognizing ability directly with 2b of series 1. Without an acridine intercalator, *i.e.*, proflavine (compounds 1) or 9-aminoacridine (compounds 2), these compounds showed very weak binding affinity towards DNA.[1]

The other type of redox-active compounds studied were cationic metalloporphyrin derivatives (Fig. 1b). DNA interactions with porphyrin and its metal complexes have been studied extensively by many researchers including ourselves.[5–9] Biological and spectroscopic results have suggested that tetrakis(4-*N*-methylpyridiniumyl)porphine (TMpyP) free base, H_2TMpyP, and the square planar complexes such as those with Cu^{2+} and Ni^{2+} intercalate between the DNA base pairs, while metalloporphyrins with axial ligands, e.g. FeTMpyP and MnTMpyP, bind to the minor groove of AT regions. Our previous study by restriction enzyme inhibition experiments as well as DNase I and micrococcal nuclease footprinting approaches suggested that porphyrins with-

*To whom correspondence should be addressed.

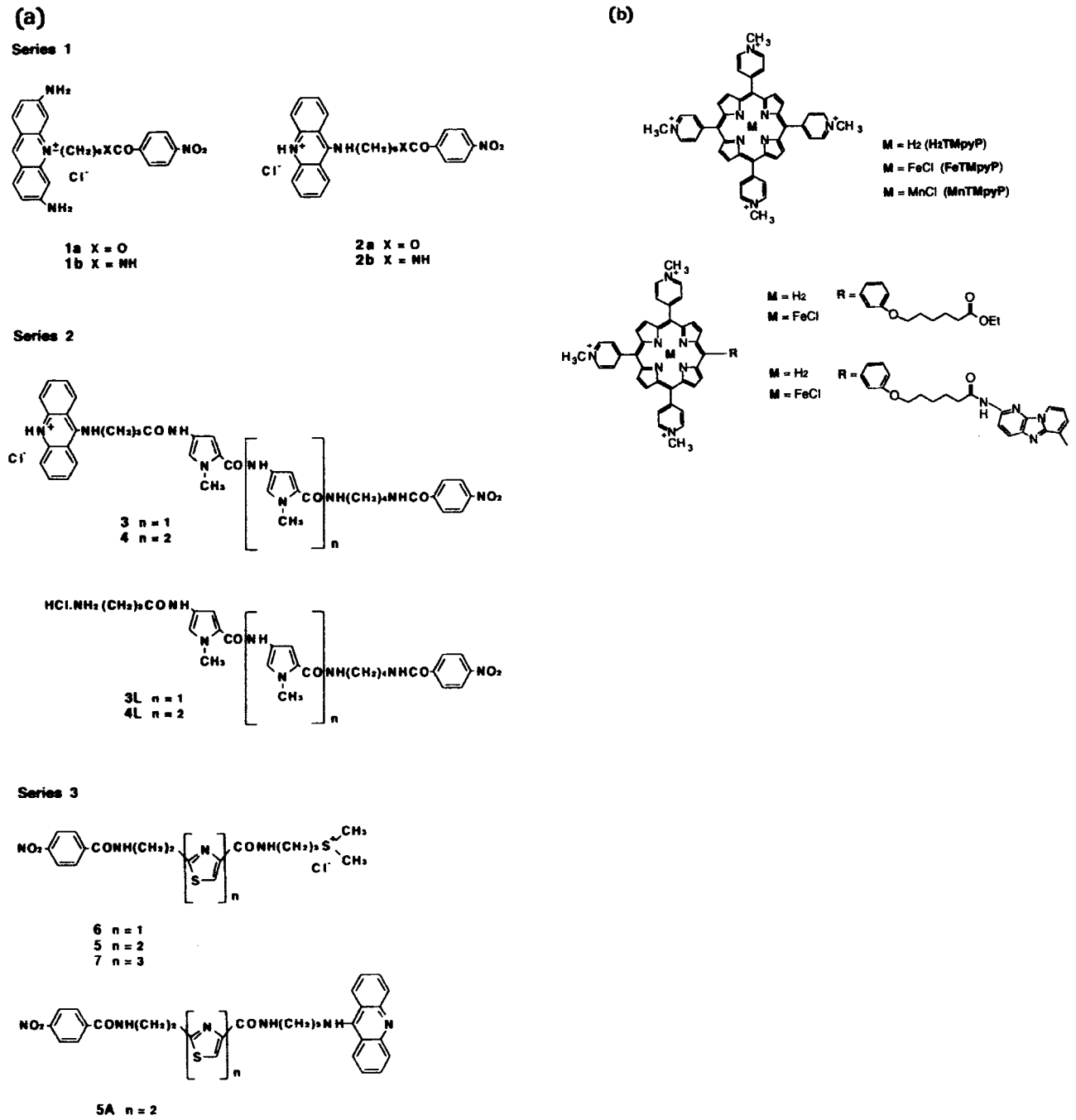

Figure 1 Structures of the photoactive(a) and redox acitive(b) compounds studied in this work.

out axial ligands display a preference towards the 5′-TAT-3′ sequence in the minor groove.[10] We have extended the work to metalloporphyrins with axial ligands, *i.e.* FeTMpyP and MnTMpyP. Fe complexes with other functional groups at the end of a long sidechain have been also studied (Fig. 1b).

In this paper we report the DNA base sequence specificity of these photoactive and redox-active compounds as studied by DNA cleavage experiments and induced CD (circular dichroism) spectroscopy (in the case of porphyrins). We discuss the origin of sequence recognition.

RESULTS

Photoactive compounds

Compounds were activated by irradiation with UV light at 310 nm which corresponds to the absorption maximum of the *p*-nitrobenzoyl group. In the absence of UV

irradiation, no photocleavage of DNA was induced by these compounds.[1,3,4] Cleavage sites on ^{32}P end-labeled DNA restriction fragments from pBR322 DNA (221 bp *Ssp*I-*Hin*d III*, 128 bp *Acc*I*—*Hin*fI) induced by the photoactive compounds were characterized by high-resolution sequencing gel electrophoresis.

A typical autoradiogram (Fig. 2a) shows sequence selective DNA cleavage by series 2 compounds as compared with little preference by 2b. Analysis of the cleavage sites by compounds 3L and 4L shows that where A/T sequences are well separated from each other by G/C sequences, the compounds appear to cleave DNA at sites 1–3 bases away from more than three contiguous (A/T) bases. The restriction fragment employed in this study was significantly A/T-rich and thus it was difficult to establish the consensus bonding/cleavage sequence for these compounds.

Fig. 2b shows a corresponding high-resolution gel obtained for the series 3 compounds using derivative 2b of series 1 as a reference. Compounds of series 3 cleaved DNA at a limited number of sites, as compared with the reference compound. The unithiazole compound, 6, (lane g) and bithiazole compound (lane f) cleaved DNA at similar sites. However, the terthiazole compound (lane h)

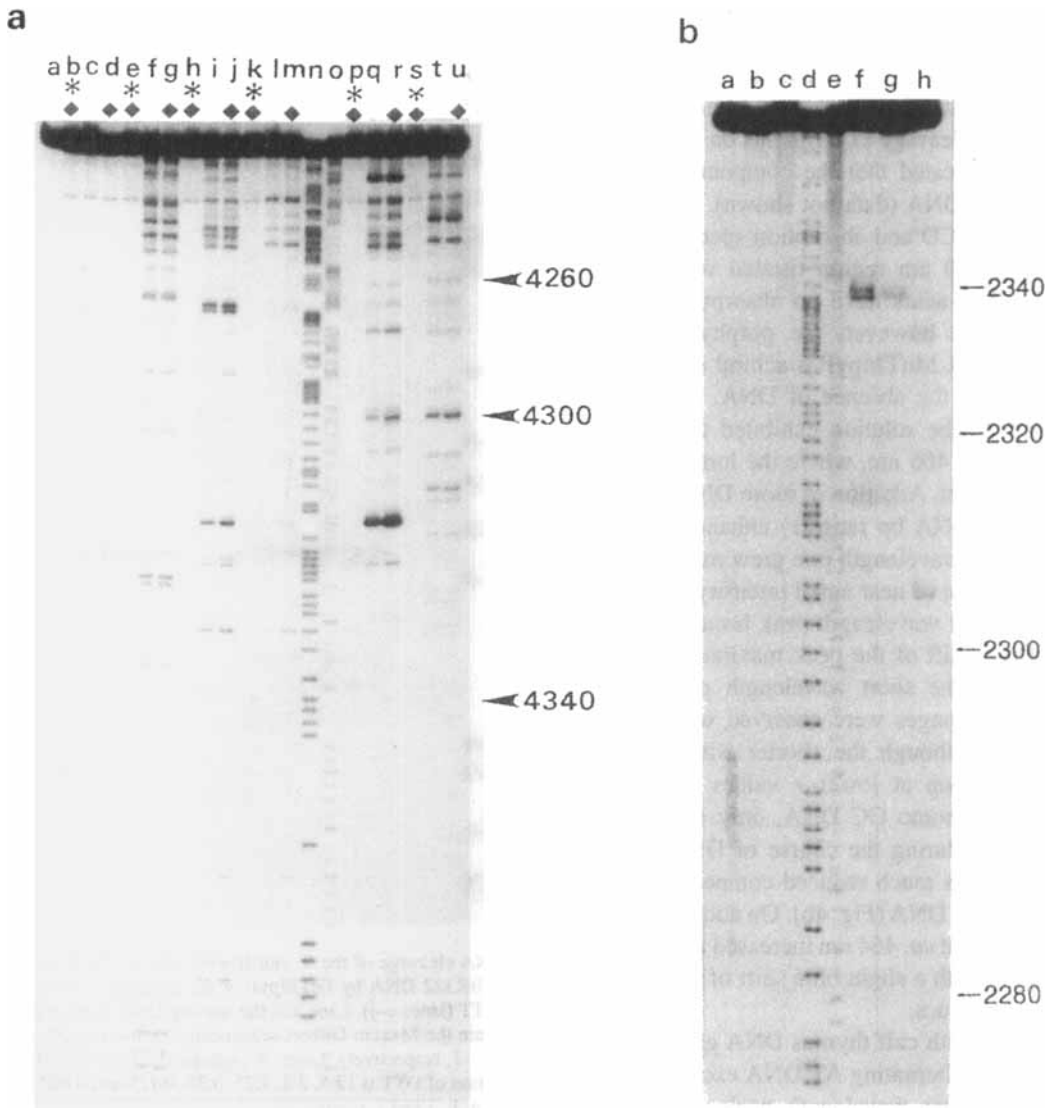

Figure 2 Cleavage of DNA by the photoactive compounds, examined by high-resolution sequencing gel electrophoresis. (a) is the autoradiogram for series 2 compounds on the 3′ end labeled 221 bp pBR322/*Ssp*I-*Hin*dIII*. * and ♦ denote no UV irradiation and treatment of the reaction mixture by 1M piperidine, respectively. Lane a is the starting DNA fragment, lanes b–d contain no drug, lane e–g **2b**, lane h–j **3**, lanes k–m **4**, lanes p–r **3L** and lane s–u **4L**. Lanes n and o are the Maxam-Gilbert sequencing reactions specific for the A+G and C+T, respectively. The concentrations of the drugs and DNA were 7.5 and 25 μM, respectively. (b) is the corresponding autoradiogram for series 3 compounds on 128 bp pBR322/*Acc*I*-*Hin*fI. All the reactions were UV irradiated. Lane a is the starting DNA fragment. Lane b contains no drug, lane c **2b**, lane f **5**, lane g **6**, and lane h **7**. Lanes d and e are the Maxam-Gilbert sequencing reactions specific for the A+G and C+T, respectively. The DNA concentration was 25 μM and the concentration of the drug was 15 μM for lane c, and 50 μM for lanes f–h.

cleaved DNA at completely different locations. The nucleotide positions of several strong cleavage sites read from the Maxam-Gilbert sequencing reactions run on the same restriction fragment revealed the consensus sequence to be 5′-AAATA-3′ for the uni- and bi-thiazole compounds.

Metalloporphyrins

The Fe porphyrins which possess a second functional group at the end of a relatively long sidechain, as well as the parent Fe complex,[11] cleaved DNA very efficiently and with the same high sequence selectivity (Fig. 3). The reactions required inclusion of reducing agent, DTT. Reading from the Maxam-Gilbert sequencing lanes on a 146 *Nhe*I*/*Bam*HI restriction fragment, cleavage occurred at the 3' side of more than three contiguous AT bases. Similar results were recently reported by Meunier's group on MnTMpyP.[12] Cleavage experiments on the opposite strand of DNA indicated that the compounds bind in the minor groove of DNA (data not shown).

Fig. 4a shows the induced CD and absorption spectra of MnTMpyP in the 420-500 nm region titrated with poly(dA-dT)$_2$ DNA. Nucleic acids have no absorption bands in the visible region, however, the porphyrin exhibits the strong Soret band. MnTMpyP is achiral and hence no CD is observed in the absence of DNA. On adding poly(dA-dT)$_2$ DNA, the solution exhibited two positive peaks at *ca.* 456 and 466 nm, where the longer wavelength peak was dominant. Addition of more DNA, *i.e.* lowering the porphyrin/DNA bp ratio (r) enhanced both peaks, though the short wavelength one grew more rapidly. The two peaks became of near equal intensity at r=*ca.* 0.4, and then the shorter wavelength peak became dominant with a slight red shift of the peak maximum. Eventually at $r \leq 0.1$ only the short wavelength peak appeared. Similar spectral changes were observed with poly(dA) · poly(dT) DNA, although the shorter wavelength peak started to develop at lower r values. In contrast, with alternating or homo GC DNA, only one positive peak was observed during the course of DNA titration, and the intensity was much reduced compared with the case of AT-containing DNA (Fig. 4b). On adding poly(dG-dC)$_2$ DNA, the peak at *ca.* 464 nm increased and then decreased in intensity with a slight blue shift of the peak maximum at lower r values.

Induced CD experiments with calf thymus DNA gave similar results to those with alternating AT DNA except that the intensity of the longer wavelength peak was relatively reduced. The two peaks observed in the case of calf thymus or AT DNA can be attributed to either of the following reasons: 1) splitting of the degenerate Bx and By bands as a result of DNA binding through a particular mode, or 2) the two peaks correspond to two different binding modes. Addition of distamycin or berenil, which

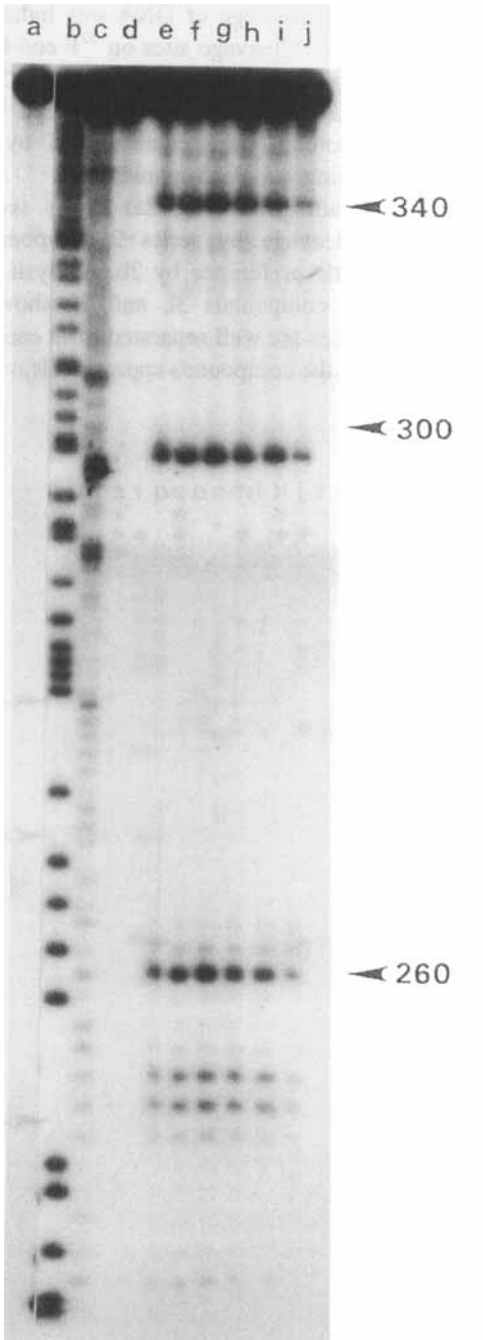

Figure 3 DNA cleavage of the 5′ end labeled 146 bp *Nhe*I*/*Bam*HI fragment of pBR322 DNA by FeTMpyP in the absence (lane d) and presence of DTT (lanes e–j). Lane a is the starting DNA fragment and lanes b and c are the Maxam-Gilbert sequencing reactions specific for the A+G and C+T, respectively. Lanes d–j contain 1.25 μM FeTMpyP. The concentration of DTT is 12.5, 2.5, 1.25, 0.25, 0.125 and 0.025 mM for lanes e, f, g, h, i and j, respectively.

are minor groove binding drugs,[3] to the solution of MnTMpyP and poly(dA-dT)$_2$ DNA, decreased the intensity of the shorter wavelength peak and at the same time increased that of the longer wavelength one. The change was more prominent at higher antibiotic concentrations.

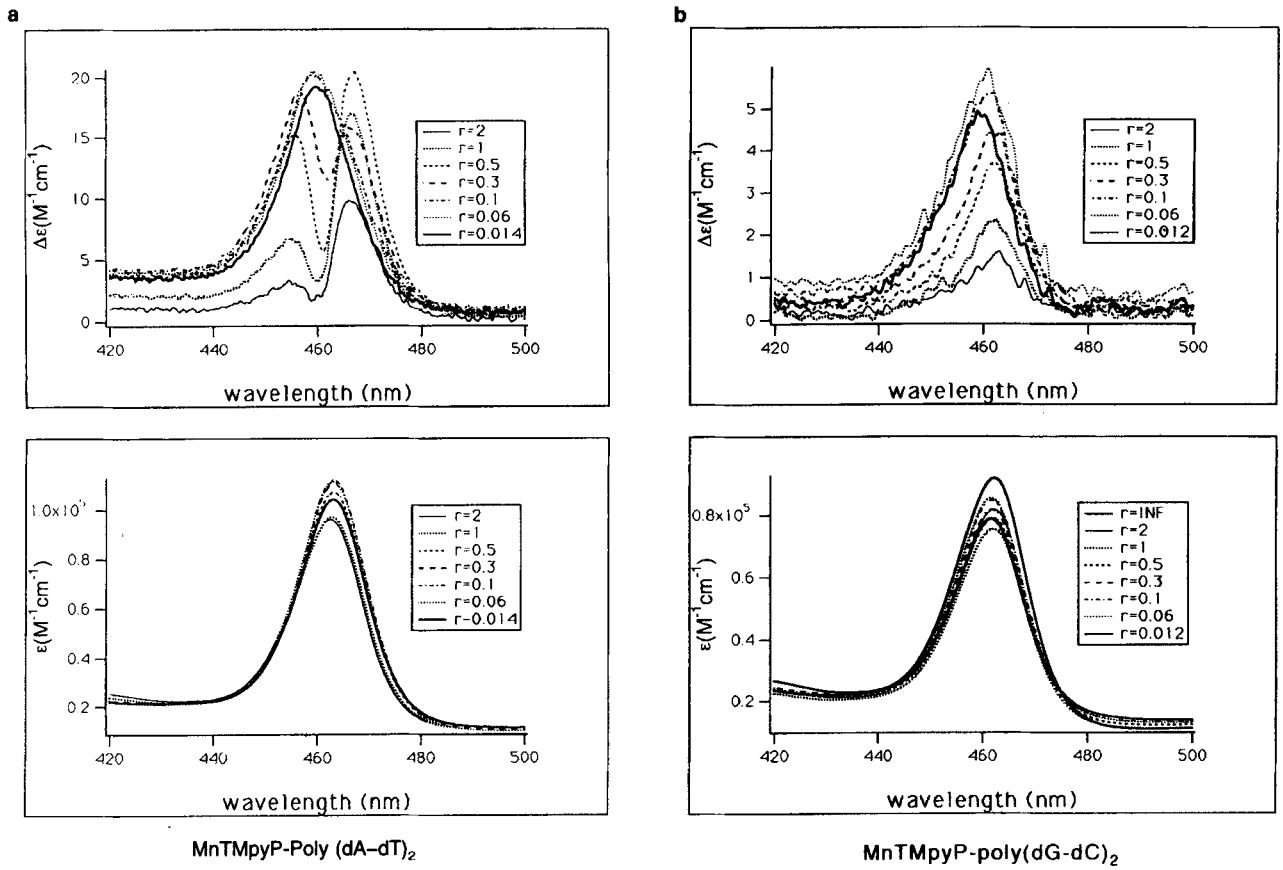

Figure 4 Induced CD(above) and absorption(below) spectra of MnTMpyP with poly(dA–dT)$_2$ (a) and poly(dG–dC)$_2$ DNA (b). For clarity only the representative curves are shown.

The likely interpretation is that preferential binding of these antibiotics to their high affinity AT sites in the minor groove of DNA displaces MnTMpyP molecules and these excluded porphyrins are then available to bind the major groove of DNA.

The single positive peak observed in the case of alternating or homo GC DNA can be assigned as a peak corresponding to the major groove binding mode, as the presence of the 2-amino group of guanine base may prevent the binding of MnTMpyP in the minor groove. This was confirmed by induced CD spectra titrated with poly(dl-dC)$_2$. These results clearly indicate that the two peaks observed in the Soret band of MnTMpyP with calf thymus, poly(dA-dT)$_2$, or poly(dA)·poly(dT) DNA correspond to two different binding modes. The shorter and the longer wavelength peaks are assigned as originating from the minor and the major groove binding modes, respectively.[13] Thus, whereas biochemical experiments revealed only the minor groove binding to AT sequences, CD studies revealed that other types of binding are not negligible.

We have carried out a mathematical analysis of the CD spectra to obtain semi-quantitative information on binding modes. Fig. 5 shows a result of curve fitting for the MnTMpyP-poly(dA-dT)$_2$ case based on either Gaussian or Lorentzian curve fitting. Assumption of two components could not explain the trough at 462 nm. However, a model with three components with Lorentzian curves gave a good fit to the experimental curve. This procedure

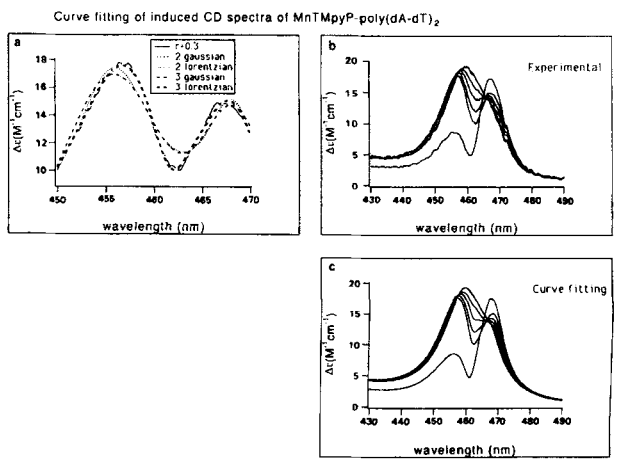

Figure 5 Curve fitting analysis of induced CD spectra for MnTMpyP–poly (dA–dT)$_2$. (a) Decomposition based on either two or three Gaussian or Lorentzian curves at r=0.3. Observed(b) and curve-fitted(c) spectra for a wide range of r values.

reproduced the spectra over a wide range of r values (Compare the observed spectra and the curve fitting in Fig. 5b and 5c).

Two out of the three components had a positive sign and were located at 458 nm and 467 nm. These peaks obviously correspond to the aforementioned peaks originating from the minor and the major groove binding, respectively. The third peak on the other hand was negative, centred at 461 nm. Using the following equation,

$$\text{Rab} = 0.124\pi\ \Delta\epsilon\ \Delta o/\lambda\text{max},$$

(where $\Delta\epsilon$ = CD peak height, Δo = half-width, and λmax = peak wavelength position), the rotatory strength, Rab, for each peak was calculated and plotted against r values in the case of MnTMpyP-poly(dA-dT)$_2$ (Fig. 6). At low r values where there are many binding sites per MnTMpyP molecule, the minor groove binding is dominant with only a minor contribution from binding in the major groove. Although the rotatory strength of the negative peak is small compared with the others and the peak appears only at higher r values, it is not negligible. We are currently studying the origin of the negative peak to determine if it arises from outside binding, partial intercalation of the porphyrin ring, interaction between bound propyrins, or major groove binding.

DISCUSSION

All the compounds examined except those of series 1 cleaved DNA with high sequence specificity. The cleavage pattern was greatly affected by the presence of the intercalating group. A preliminary binding model for compounds 3L and 4L without the intercalator is shown in Fig. 7. This is based on X-ray crystallographic studies of netropsin-d(CGCGAATTCGCG)$_2$,[14] netropsin-d(CGCGATATCGCG)$_2$[15] and distamycin-d(CGCAAATTTGCG)$_2$ complexes.[16] The drug is held in place within the minor groove of DNA by amide NH hydrogen bonds that bridge adenine N-3 and thymine 0-2 atoms. The excited triplet state formed upon irradiation of the aromatic nitro group is known to abstract hydrogen from a sugar carbon atom to which an oxygen atom is also bonded, leading to DNA strand breakage.[17] Our model building studies have shown that the nitro group can approach sugar hydrogen atoms at a maximum of three bases away from the last A/T base recognized by the amide hydrogen atoms, which is in relatively good agreement with the observed cleavage pattern. A preference for AT sequences was confirmed by DNase I footprinting work which will be reported elsewhere.

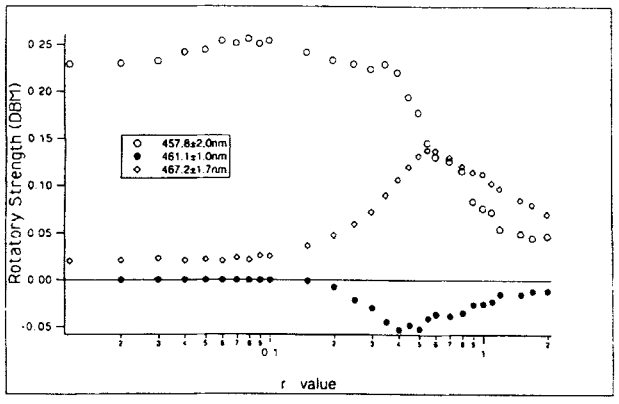

Figure 6 Rotatory strengths of the three component peaks plotted against r values for the case of MnTMpyP-poly(dA-dT)$_2$ DNA.

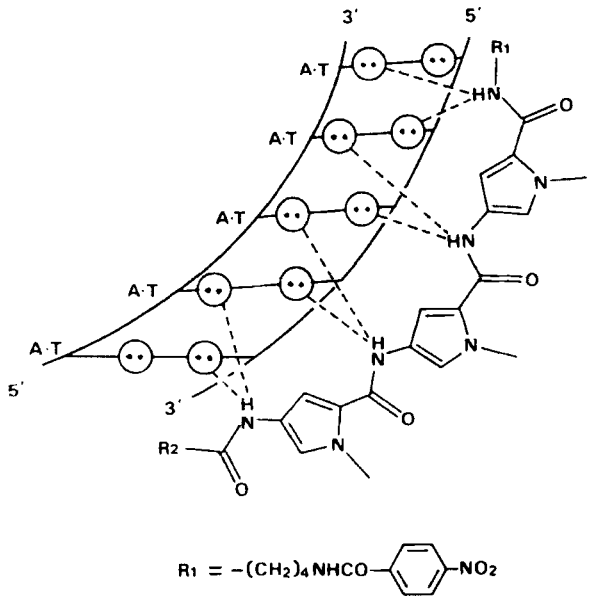

Figure 7 A DNA binding model for compounds **3L** and **4L**.

Series 3 compounds with thiazole units are markedly sequence specific. Compound 5 can be regarded as the DNA binding portion of bleomycin A_2, to which the photoactive p-nitrobenzoyl group has been covalently linked. Fig. 8 shows the structure of bleomycin A_2. Bleomycin antitumour antibiotics are composed of two

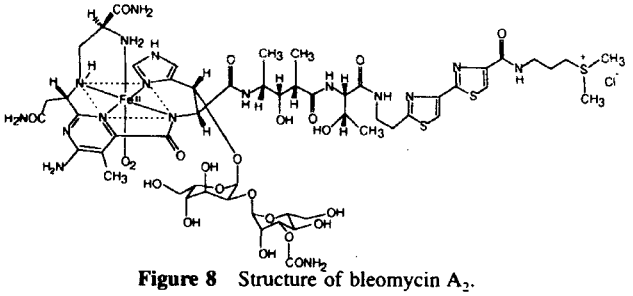

Figure 8 Structure of bleomycin A_2.

functionally distinct domains, *i.e.* a moiety which is responsible for chelating of the required metal cofactor e.g. Fe(II), and the DNA binding region, *i.e.* 4-(3-dimethylsulfoniuopropylaminocarbonyl)-bithiazole group. Bleomycins induce DNA scission at limited sites with preference for 5′-GpT-3′ and 5′-GpC-3′ sequences, and their antitumour activity is thought to stem from their ability to cleave DNA. The bithiazole group has been considered to be largely or solely responsible for the sequence selectivity of its DNA interactions[18]. Contrary to what is expected, scission by 5 did not occur at or near GpT or GpC sites. These results, as well as the relatively weak DNA binding affinity of the oligothiazole group suggested by the photocleavage experiments indicate that bleomycin-induced specific scission is not solely determined by the bithiazole terminus. This agrees with recent reports by Haseltine,[19] Hecht[20] and Fox[21] who have independently questioned the role of the bithiazole unit in sequence recognition by bleomycins. We are presently carrying out studies using computer graphics as well as fluorescence to investigate the DNA binding mode of the thiazole group. Attachment to the photoactive *p*-nitrobenzoyl group appears to be useful in identifying the sequence specificity of DNA binding ligands.

Affinity cleavage experiments revealed that FeTMpyP breaks DNA at a limited number of sites, suggesting that metalloporphyrins with axial ligands exhibit high sequence specificity. This is somewhat surprising as these compounds do not contain any functional group capable of hydrogen bonding, a determinant of specificity in many DNA-ligand recognitions. From detailed analysis of induced CD spectroscopy, we could show that metalloporphyrins exhibit rather complex DNA binding involving not only the minor groove of AT sequences as revealed by biochemical experiments but also the major groove of AT or GC sequences. The preferred binding mode depends on *r*, the porphyrin/DNA bp ratio. FeTMpyP and MnTMpyP may cleave DNA only when they interact with DNA through a particular binding mode, although other binding modes take place at the same time. The preferred orientation for DNA cleavage in this case is in the minor groove of more than three contiguous AT basepairs. The extremely high specificity observed must be achieved by a specific orientation of the molecules within the groove. One possible source of this recognition is electrostatic interactions between the positive charges on the nitrogen atoms of the porphyrin and the negative phosphate oxygens of DNA. To assess this possibility we are currently making metalloporphyrins with reduced numbers of positive charges.

We have assigned CD peaks of MnTMpyP induced by binding to the chiral environment of DNA. CD is highly sensitive to the electronic environment. During titration with synthetic and natural DNAs, the absorption spectra of MnTMpyP exhibited only a minor change in contrast to the corresponding CD spectra (Fig. 4). These results clearly illustrate the power of induced CD spectroscopy. Mathematical analysis of induced CD spectra provides further information which is not obtainable from simple visual inspection.

In this study, we have designed and synthesized a variety of photoactive and redox active DNA cleaving compounds which display high sequence specificity. The mechanism of sequence recognition appears to be quite different in the two cases. This work has shown that the combination of spectroscopic and biochemical approaches can provide unique and detailed information on the sequence-specific nature of DNA-ligand binding.

MATERIALS AND METHODS

A preliminary account of the synthesis of the compounds has been reported[1,3,22] except some porphyrins which will be reported elsewhere.

Polynucleotide kinase and restriction enzymes, *Bam*HI, *Hin*dIII and *Hinf*I were purchased from Takara Shuzo Co., Ltd. Restriction enzymes *Acc*I, *Nhe*I and *Ssp*I were purchased from New England Biolabs, Inc. AMV reverse transcriptase and micrococcal nuclease were from Pharmacia LKB Biotechnology. Synthetic polymer and calf thymus DNA were from Sigma.

Plasmid pBR322 DNA was isolated from *Escherichia coli* strain MG1182 by Triton lysis and was purified by banding twice in CsCl-ethidium bromide gradients as previously described.[23] Ethidium bromide was removed by several 1-butanol extractions followed by exhaustive dialysis.[23]

^{32}P end-labeled DNA fragments

Restriction fragments from plasmid pBR322 were used for the analysis of DNA cleavage. The 128 base pair *Acc*I*-*Hinf*I restriction fragment from pBR322 labeled at the 5′ *Acc*I end was prepared as follows. pBR322 DNA (10 μg) was linearized with *Acc*I and then treated with alkaline phosphatase for 60 min at 37°C. Following phenol extraction and ethanol precipitation, the DNA was labeled by incubation with T4 polynucleotide kinase (5 units) and [γ-^{32}P]ATP (3.7 MBq) in 5 mM Tris-HCl, 5 mM KCl, 0.1 mM DTT, pH 7.5 at 37°C for 30 min. The DNA was precipitated with ethanol, digested with *Hinf*I, and run on a 2% low gelling agarose gel in TBE buffer (89 mM Tris base, 89 mM boric acid, 2.5 mM Na_2EDTA). The 128-bp *Acc*I-*Hinf*I band was identified by autoradiography, excised and isolated by phenol extraction. The fragment was purified by ethanol precipitation. The other 5′-end labeled restriction fragment was prepared similarly.

The 3'-end labeled fragment was prepared by first linearizing pBR322 (10 μg) with *Hin*dIII and then labeling with AMV reverse transcriptase (47.5 units) and [α-^{32}P] dATP in 50 mM Tris-HCl, pH 8.3, 40 mM KCl, 6 mM $MgCl_2$ and 6 mM 2-mercaptoethanol at 37°C for 2 hrs. The DNA was precipitated with ethanol, and digested with *Ssp*I. The required fragments were isolated and purified as for the 5'-end labeled DNA.

MAPPING OF DNA CLEAVAGE SITES

Photocleavage agents

Reaction mixtures (total volume 3.0 μl) containing 3 mM Tris-HCl/0.03 mM EDTA, pH 7.5, 25 μM (in base-pairs) calf thymus DNA, the end labeled DNA restriction fragment and the desired concentration of photocleavage agent were preincubated for 30 min at room temperature. Each reaction mixture in an Eppendorf tube was irradiated with a mercury lamp (UVP, model TM20, 90W) for 90 min at a distance of 15 cm. Two filters—a plastic plate (Falcon) and a 1 M $NiSO_4$ solution (1 cm path-length)—were used to obtain *ca.* 310 nm light, which roughly corresponds to the n–π* transition of the aromatic nitro group. Samples were treated with 1 M piperidine and heated for 8 min at 90°C. The reaction mixture was lyophilized and dissolved in 2 μl sequencing dye-mix (80% deionized formamide, 50 mM Tris-borate, 1 mM EDTA, 1% bromophenol blue), and heated to 90°C for 4 min before loading and electrophoresis in a 10% polyacrylamide/8 M urea denaturing gel. G+A and C+T chemical sequencing reactions were carried out according to the method of Maxam & Gilbert.[24] Autoradiography was at −70°C with Fuji RX X-ray film and a light intensifying screen.

Metalloporphyrins

Reaction mixtures (total volume 3.0 μl) containing 3 mM Tris-HCl/0.03 mM EDTA, pH 7.5, 25 μM (in base-pairs) calf thymus DNA, the end labeled DNA restriction fragment and the Fe porphyrin complexes (1.25 μM) were preincubated for 30 min at room temperature. After incubation at 37°C for 10 min with various concentration of DTT, the reaction mixture was lyophilized and dissolved in 2 μl sequencing dye-mix (80% deionized formamide, 50 mM Tris-borate, 1 mM EDTA, 1% bromophenol blue), and heated to 90°C for 4 min before loading and electrophoresis in a 10% polyacrylamide/8 M urea denaturing gel. G+A and C+T chemical sequencing reactions were carried out according to the method of Maxam & Gilbert.[24] Autoradiography was at -70°C with Fuji RX X-ray film and a light intensifying screen.

Spectroscopy

Absorption spectra of MnTMpyP were measured on Beckman DU64 and Shimazu UV-2200 spectrometers. CD spectra were recorded on a Jasco J-720 spectropolarimeter in 25 mmol dm^{-3} phosphate buffer (pH 7.1).

ACKNOWLEDGMENT

The authors are grateful to the Ministry of Education (Grant-in-Aid for Scientific Research; B:01470047, A:03403009, Bioinorganic:04225205) as well as Nissan Science Foundation for the financial support (to R.K.).

REFERENCES

1 Kuroda, R.; Shinomiya, M.; *Biochem. Biophys. Res. Commun.* **1991**, 181, 1266.
2 Zimmer, C.; Wähnert, U.; *Prog. Biophys. Molec. Biol*, **1986**, 47, 31.
3 Shinomiya, M.; Kuroda, R.; *Tetrahedron Lett.* **1992**, 33, 2697.
4 Kuroda, R; Shinomiya, M.; Otsuka, M.; *Nucleic Acids Symp. Ser.* **1992**, 27, 9.
5 Fiel, R.J.; Howard, J.C.; Mark, E.H.; Datta-Guputa, N.; *Nucleic Acids Res.* **1979**, 6, 3093.
6 Pasternack. R.F.; Gibbs, E.J.; Villafranca, J.J.; *Biochemistry* **1983**, 22, 2406.
7 Ward, C.B.; Skorobogaty, A.; Dabrowiak, J.C.; *Biochemistry* **1986**, 25, 7827.
8 Review: Marzilli, L.G.; *New J. Chem.* **1990**, 14, 409, and references therein.
9 Kuroda, R.; Takahashi, E.; Austin, C.A.; Fisher, L.M.; *FEBS Lett.* **1990**, 262, 293.
10 Watanabe, S.; Kuroda, R.; Furubayashi, M.; to be submitted.
11 Kuroda, R.; Tanaka, H.; Watanabe, S.; *Nucleic Acids Symp. Ser.* **1993**, 29, 123.
12 Pietié, M.; Partiviel; G.; Bernadou, J.; Muenier, B.; *Proc. Natl. Acad. Sci. U.S.A.* **1992**, 89, 3967.
13 Kuroda, R.; Tanaka, H.; *J. Chem. Soc. Chem. Commun.* **1994**, 1575.
14 Kopka, M.L; Yoon, C.; Goodsell, D.; Pjur, P.; Dickerson, R.E.; *Proc. Natl. Acad. Sci. U.S.A.* **1985**, 82, 1376.
15 Coll, M.; Aymami, J.; van der Marel, G.A.; van Boom, J.H.; Rich, A.; Wang, A.H.-J.; *Biochemistry* **1989**, 28, 310.
16 Coll. M.; Frederick, C.A.; Wang, A.H.-J.; Rich, A.; *Proc. Natl. Acad. Sci. U.S.A.* **1987**, 84, 8385.
17 Nielsen, P.E.; Jeppesen, C.; Egholm, M.; Buchardt, O.; *Biochemistry* **1988**, 27, 6338.
18 Stubbe, J.; Kozarich, J.W.; *Chem. Rev.* **1987**, 87, 1107 and references therein.
19 Kross, J., Henner, W.D., Hecht, S.M. & Haseltine, W.A.; *Biochemistry* **1982**, 21, 4310.
20 Carter, B.J.; Reddy, K.S.; Hecht, S.M. *Tetrahedron* **1991**, 47, 2463.
21 Nightingale, K.P.; Fox, K.R.; *Nucleic Acids Res.* **1993**, 21, 2549.
22 Kobayashi, S.; Kuroda, R.; Watanabe, T; Otsuka, M.; *Synlett.* **1992**, 59.
23 Sakakibara, Y.; Tomizawa, J.; *Proc. Natl. Acad. Sci. U.S.A.* **1974**, 71, 802.
24 Maxam, A.M.; Gilbert, W.; *Proc. Natl. Acad. Sci. U.S.A.* **1977**, 74, 560.